Beam Systematics for Mott Experiment Runs I and II

Joe Grames and Brian Freeman

February 22, 2017
JLab-TN-17-007

Abstract

Systematic studies of the Mott experimental asymmetry to electron beam conditions such as beam position, beam size, and energy spread measured during Runs I and II are summarized in this note.

1 Introduction

Beam Lines

A schematic of the relevant beam components is shown in Fig. 1. Quads MQJ0L02/MQJ0L02A varies beam size and SRF cavity phase R028PSET varies energy spread. Wire scanners IHA0L03 and IHA2D00 are used to determine emittance/Twiss at MQJ0L02 and momentum spread, respectively. The Mott targets are viewed by camera ITV3D01.

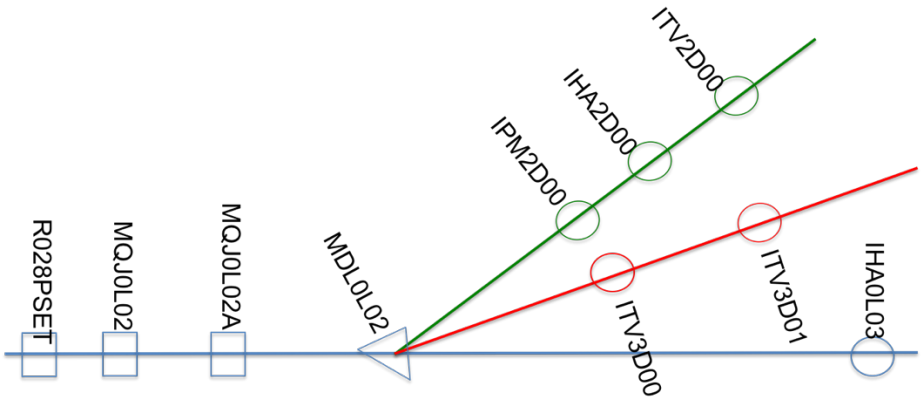

Fig. 1. Dipole MDL0L02 deflects beam to the Mott (red) or Spectrometer (green).

Elegant Model

An Elegant model beginning at MQJ0L02 and ending at IHA2D00 or ITV3D01 was designed.

```
"cle" ! clear whole RPN stack for safety

% 1 atan 4 * sto pi
% pi 180 / sto cdtor
% 180 pi / sto crtod

! DRIFT BETWEEN QUADS
D1      : DRIFT, L=0.4596

! DRIFT TO 2D LINE
D2      : DRIFT, L=1.0065
D3      : DRIFT, L=3.1385
D4      : DRIFT, L=0.1778
D5      : DRIFT, L=0.1270
```

```
! DRIFT TO 3DLINE
D6      : DRIFT, L=1.0041
D7      : DRIFT, L=0.5584
D8      : DRIFT, L=0.2667
D9      : DRIFT, L=0.8113

! NORMAL MOTT
MQJ0L02:  KQUAD, L=0.15, K1= -5.04003396226415
MQJ0L02A: KQUAD, L=0.15, K1= +5.00232327044025

! 2D DIPOLE
MDL0L02_2D: CSBEND, L=0.1230, ANGLE="-30.0 180.0 / -1 acos * ", &
      E1=" 0.0 180.0 / -1 acos * ", E2="-30.0 180.0 / -1 acos * ", &
      EDGE_ORDER=2, HGAP=0.013564, FINT=0.5, NONLINEAR=1, &
      N_KICKS=15, INTEGRATION_ORDER=4

! 3D DIPOLE
MDL0L02_3D: CSBEND, L=0.1278, ANGLE="-12.5 180.0 / -1 acos * ", &
      E1=" 0.0 180.0 / -1 acos * ", E2="-12.5 180.0 / -1 acos * ", &
      EDGE_ORDER=2, HGAP=0.013564, FINT=0.5, NONLINEAR=1, &
      N_KICKS=15, INTEGRATION_ORDER=4

! DIAGNOSTIC IN 2D LINE
IPM2D00: WATCH, FILENAME="%s.ITV2D00", MODE=COORD
ITV2D00: WATCH, FILENAME="%s.ITV2D00", MODE=COORD
IHA2D00: WATCH, FILENAME="%s.IHA2D00", MODE=COORD

! DIAGNOSTIC IN 3D LINE
ITV3D00: WATCH, FILENAME="%s.ITV3D00", MODE=COORD
ITV3D01: WATCH, FILENAME="%s.ITV3D00", MODE=COORD

! BEAM LINES
2D:  LINE=(MQJ0L02, D1, MQJ0L02A, D2, MDL0L02_2D, D3, IPM2D00, D4, IHA2D00, D5,
ITV2D00)
3D:  LINE=(MQJ0L02, D1, MQJ0L02A, D6, MDL0L02_3D, D7, D8, ITV3D00, D9, ITV3D01)
```

2 Run I Results

Run I Energy

The electron kinetic energy reported in [1] is 4.806 ± 0.097 MeV corresponding to a momentum of 5.292 ± 0.098 MeV/c.

Run I Beam Emittance

Horizontal and vertical beam projections at wire scanner IHA0L03 were measured as a function of MQJ0L02 strength using *qsUtility 3.21* (see Fig. 2). The emittance and Twiss are calculated by *sddsemitproc* and reported in e3466292 and summarized in Table 1.

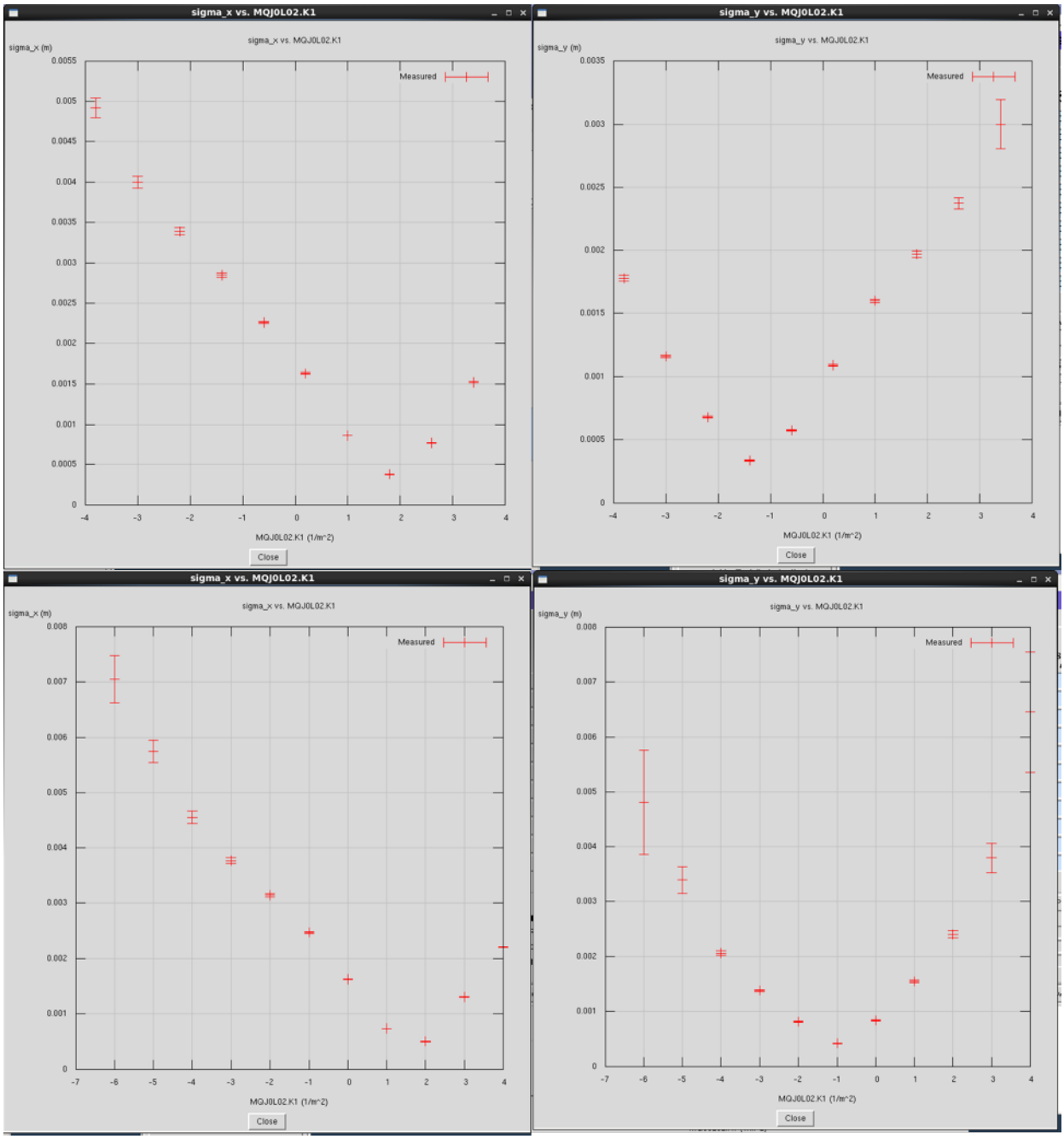

Fig. 2. Upper (lower) plots show plots of beam size measured at IHA0L03 as a function of quad strength MQJ0L02 taken at 2015-01-18_22:36 (IHA0L03_2015-01-19_17:15).

Table 1. Summary of measured normalized emittance and Twiss parameters at MQJ0L02.

qsUtility (run date)	$\varepsilon_{n,x}$ (μm)	β_x (m)	α_x (rad)	$\varepsilon_{n,y}$ (μm)	β_y (m)	α_y (rad)
2015-01-18_22:36	0.534(3)	15.8(1)	-2.01(2)	0.342(2)	13.3(5)	-0.617(11)
2015-01-19_17:15	0.593(5)	14.4(2)	-1.42(3)	0.461(2)	11.2(2)	-0.070(06)

Run I : Asymmetry vs. Beam Energy Spread

The Mott asymmetry as a function of energy spread was studied by varying the phase R028PSET of the last SRF cavity before the polarimeter about the nominal set point. The beam energy spread is determined from a measurement of the beam size at a dispersive location according to

$$S_x^2 = \varepsilon_x \beta_x + \left(\frac{dp}{p}\,\eta_x\right)^2$$

where S_x is the horizontal RMS beam size. The horizontal dispersion function is calculated at the wire scanner IHA2D00 η_x = -1.946 m and at the Mott target ITV3D01 η_x = -0.3767 m. For each value of R028PSET the beam size at IHA2D00 [IHA2D00_2015-01-19_*] (see Fig. 3) and the Mott asymmetry using foil #15 (Au:1 μm) were measured and summarized in Table 2.

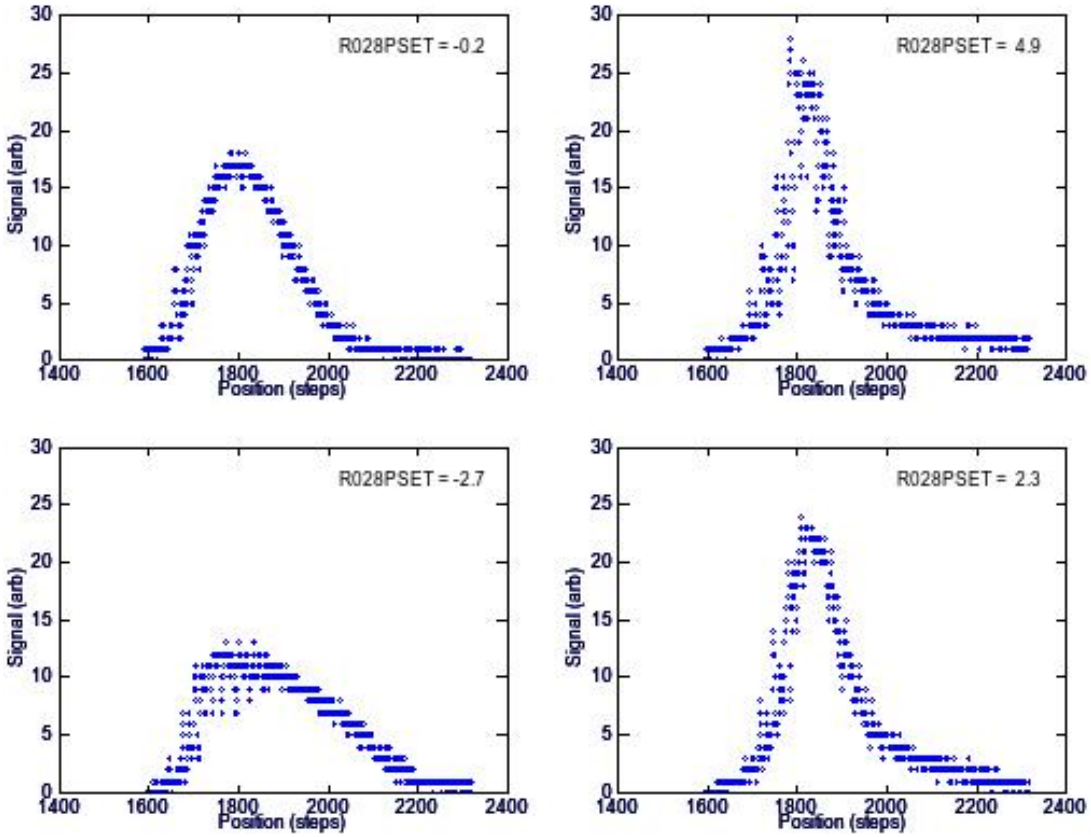

Fig. 3. The horizontal wire scanner signal as a function of motor position for four values of R028PSET are shown. The wire scanner reports a position calibration of 0.02041 mm/step.

Using the measured emittance (2015-01-19_17:15) and recorded quadrupole strengths MQJ0L02 = -133.65 G (K = -5.048 m^{-1}) and MQJ0L02A = 132.95 G (K = 5.010 m^{-1}) yields a beam size without dispersive effects at harp IHA2D00 of 0.21 mm. The relative momentum spread ($\delta p/p$) and corresponding energy spread (δT) are summarized in Table 2 and plotted versus phase offset in Fig. 4. A plot of the Mott run physics asymmetries versus phase offset and energy spread is plotted in Fig. 5. Note, the horizontal and vertical RMS beam size at Mott target including energy spread is computed using Elegant and reported in Table 2. The spot diameter is computed as the ellipsoidal quadratic mean diameter and the largest value of the four cases is 0.63 mm.

Table 2. Parameters and results of energy spread measurements.

R028-PSET	Δ-PSET	R028 GSET	MAD 3D00H	Mott		File	S_x (RMS) IHA2D00		δp/p	δT	Sx Mott	Sy Mott
deg	deg	MV/m	G-cm	IN	OUT		steps	mm	10^{-3}	keV	mm	mm
-0.2	0.0	4.81	0	8180	8181	22:55	76.00	1.55	0.79	3.46	0.76	0.37
4.8	-5.0	4.82	20	8182	8183	22:44	136.29	2.78	1.00	4.41	0.80	0.38
-2.7	2.5	4.81	-9	8184	8185	22:53	137.63	2.81	1.02	4.45	0.80	0.38
2.3	-2.5	4.81	11	8186	8187	22:51	118.55	2.42	0.87	3.83	0.78	0.38

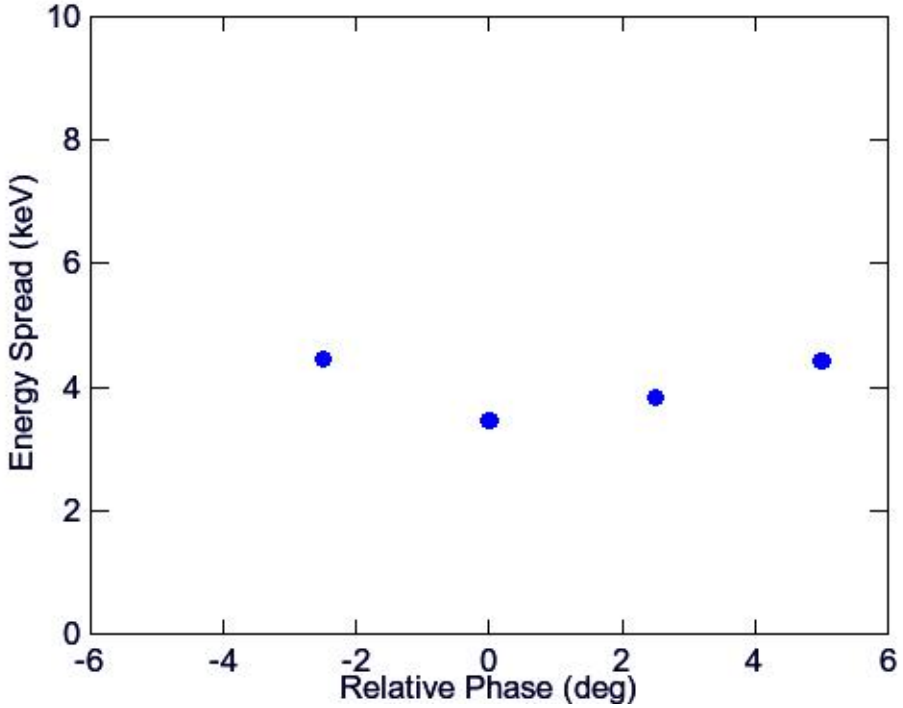

Fig. 4. The computed energy spread as a function of relative phase of second SRF cavity about the value used for Run 1 (R028PSET = -0.2 deg).

Run I: Asymmetry vs. Beam Spot Size

The Mott asymmetry as a function of beam spot size was studied by varying the quad strengths MQJ0L02 and MQJ0L02A about their nominal operating set points. For each case the Mott asymmetry using foil #15 (Au:1 μm) was measured with about 2 μA of beam current. The predicted horizontal and vertical RMS spot size using emittance (2015-01-19_17:15) and relative momentum spread (7.9 x 10^{-4}) is summarized in Table 3. Runs in bold have visually poor spectra and are not included in final analysis. A plot of the Mott run physics asymmetries versus spot size is plotted in Fig. 6. The spot diameter is computed as the ellipsoidal quadratic mean diameter (see Appendix B). The RMS asymmetry for spot size less than 1 mm is 0.3380.

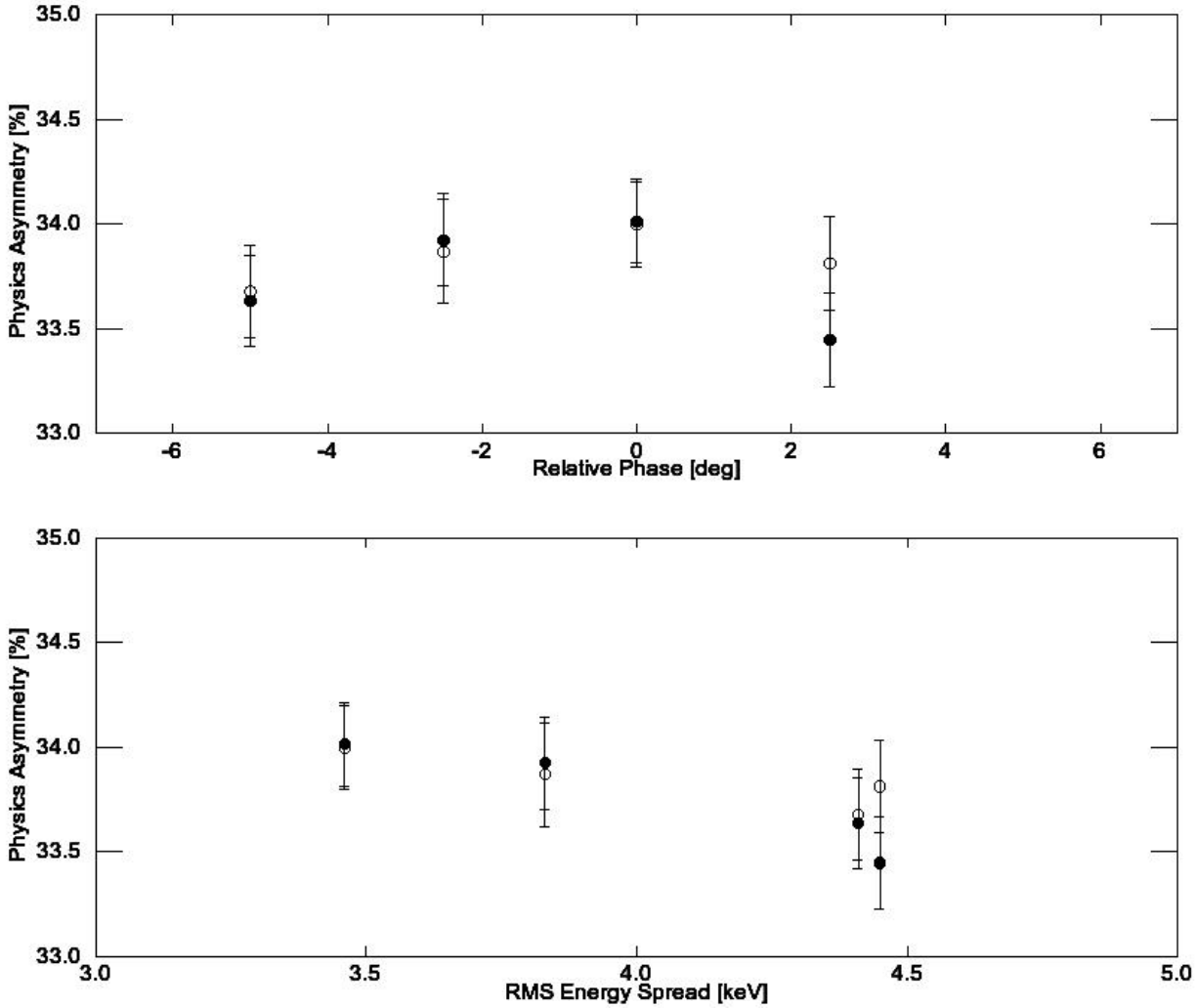

Fig. 5. Physics asymmetry versus relative phase (top) and RMS energy spread (bottom).

Table 3. Summary of spot size measurements. "Name" is estimated size during Run I and "Fig." corresponds to the OTR image in e3318205. Runs with visually bad spectra are in **bold**.

Name (mm)	Fig.	MQJ0L02		MQJ0L02A		IHWP IN	IHWP OUT	Sx	Sy
		G	1/m	G	1/m			mm	mm
0.100	1	-133.00	-5.0231	153.00	5.7785	8163	8164	**0.40**	**0.30**
0.250	2	-115.00	-4.3433	139.00	5.2497	8165	8166	**0.47**	**0.23**
0.500	3	-164.00	-6.1939	153.00	5.7785	8167	8169	**0.66**	**0.68**
1.000	4	-188.00	-7.1003	141.00	5.3252	**8170**	**8171**	**1.17**	**1.05**
2.000	5,6	-264.00	-9.9707	130.00	4.9098	**8172**	**8173**	**2.34**	**2.10**
0.750	7	-182.00	-6.8737	148.00	5.5896	8174	8175	**0.94**	**0.94**
1.500	8,9	-225.00	-8.4977	135.00	5.0986	**8176**	**8177**	**1.74**	**1.57**
0.475	10	-133.65	-5.0477	132.65	5.0099	8178	8179	**0.76**	**0.38**

Run I: Asymmetry vs. Beam Position

The Mott asymmetry as a function of beam position was studied by varying two upstream steering coils MBH0L01AH and MBH0L01AV. The beam was positioned at 6 locations within about one spot size of the nominal position. For each position the Mott physics asymmetry was measured using both foil #15 (Au:1μm) e3318095 with about 2 μA and foil #1 (Au:0.225 μm) e3318137 with about 4 μA and an OTR image of the beam from the foil was recorded. The predicted beam positions are summarized in Table 4. Plots of the Mott physics asymmetry versus beam position is shown for both targets in Fig. 7.

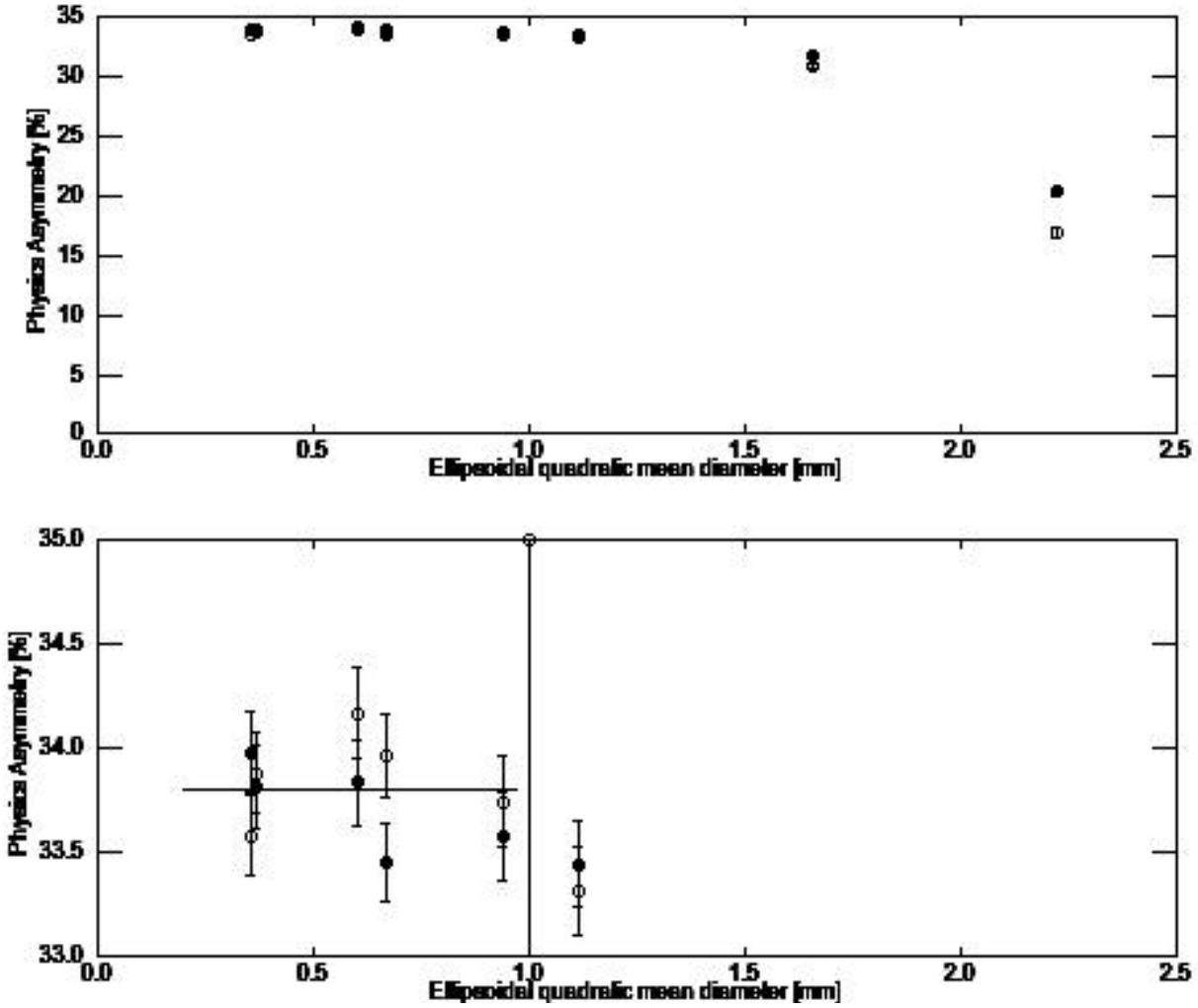

Fig. 6. Physics asymmetry as a function of the beam size for all runs (top) and for runs with good spectra (bottom).

Three steps are applied to determine the beam position at the foil from the OTR camera images:

- Using *ImageJ* the raw PNG image files are processed to determine a similar bounding box of 165 x 165 pixels on each image within 2 px. The centroid of the OTR profile is computed within the horizontal and vertical camera reference frame,

- The camera coordinates are transformed to the target coordinates. The transformation (see Appendix A for details) between the (c)amera pixels and the (b)eam pixels is given by:

$$\begin{pmatrix} x_b \\ y_b \end{pmatrix} = \begin{pmatrix} -0.579 & -0.579 \\ -0.819 & 0.595 \end{pmatrix} \begin{pmatrix} x_c \\ y_c \end{pmatrix}$$

- By taking images of the ladder for known linear vertical motion a calibration of transformed pixels to real vertical motion is determined to be 37.9 px/mm.

Table 4. Summary of position measurements.

Foil	Motion		MBH0L01A Relative		Image	Mott Run		Image Pixels		Image Rel Pixels		Foil Rel Pixels		Foil Rel (mm)		
	Real	OTR	Hor	Ver		IN	OUT	X	Y			X	Y	X	Y	R
15	0	0	0	0	run1-foil15-fig7.png	8132	8131	80.2	93.2	0.0	0.0	0.0	0.0	0.0	0.0	0.0
15	U	U	0	30	run1-foil15-fig5.png	8134	8133	61.9	107.5	-18.4	14.3	2.4	23.5	0.1	0.6	0.6
15	D	D	-0.2	-30	run1-foil15-fig6.png	8136	8135	99.4	75.8	19.1	-17.4	-1.0	-26.0	0.0	-0.7	0.7
15	R	L	29.8	0	run1-foil15-fig8.png	8138	8137	65.2	78.6	-15.1	-14.6	17.2	3.7	0.5	0.1	0.5
15	L	R	-30	0	run1-foil15-fig9.png	8140	8139	97.4	109.8	17.2	16.6	-19.5	-4.2	-0.5	-0.1	0.5
15	LD	RD	-30	-30	run1-foil15-fig10.png	8142	8141	114.5	95.2	34.3	2.0	-21.0	-26.9	-0.6	-0.7	0.9
15	RU	LU	30	30	run1-foil15-fig11.png	8144	8143	46.4	97.0	-33.9	3.8	17.4	30.0	0.5	0.8	0.9
1	0	0	0	0	run1-foil1-fig3.png	8146	8145	86.0	95.4	0.0	0.0	0.0	0.0	0.0	0.0	0.0
1	LD	RD	-30	-30	run1-foil1-fig4.png	8149	8147	121.2	92.8	35.1	-2.6	-18.8	-30.3	-0.5	-0.8	0.9
1	LU	RU	-30	30	run1-foil1-fig5.png	8151	8150	83.7	125.2	-2.3	29.8	-15.9	19.6	-0.4	0.5	0.7
1	RU	LU	30	30	run1-foil1-fig6.png	8153	8152	52.1	99.4	-34.0	4.0	17.3	30.2	0.5	0.8	0.9
1	RD	LD	30	-30	run1-foil1-fig8.png	8155	8154	86.2	62.6	0.2	-32.8	18.8	-19.7	0.5	-0.5	0.7
1	D	D	0	-30	run1-foil1-fig9.png	8157	8156	102.4	78.8	16.3	-16.6	0.1	-23.2	0.0	-0.6	0.6
1	L	R	-30	0	run1-foil1-fig10.png	8159	8158	101.7	106.8	15.7	11.4	-15.7	-6.0	-0.4	-0.2	0.4

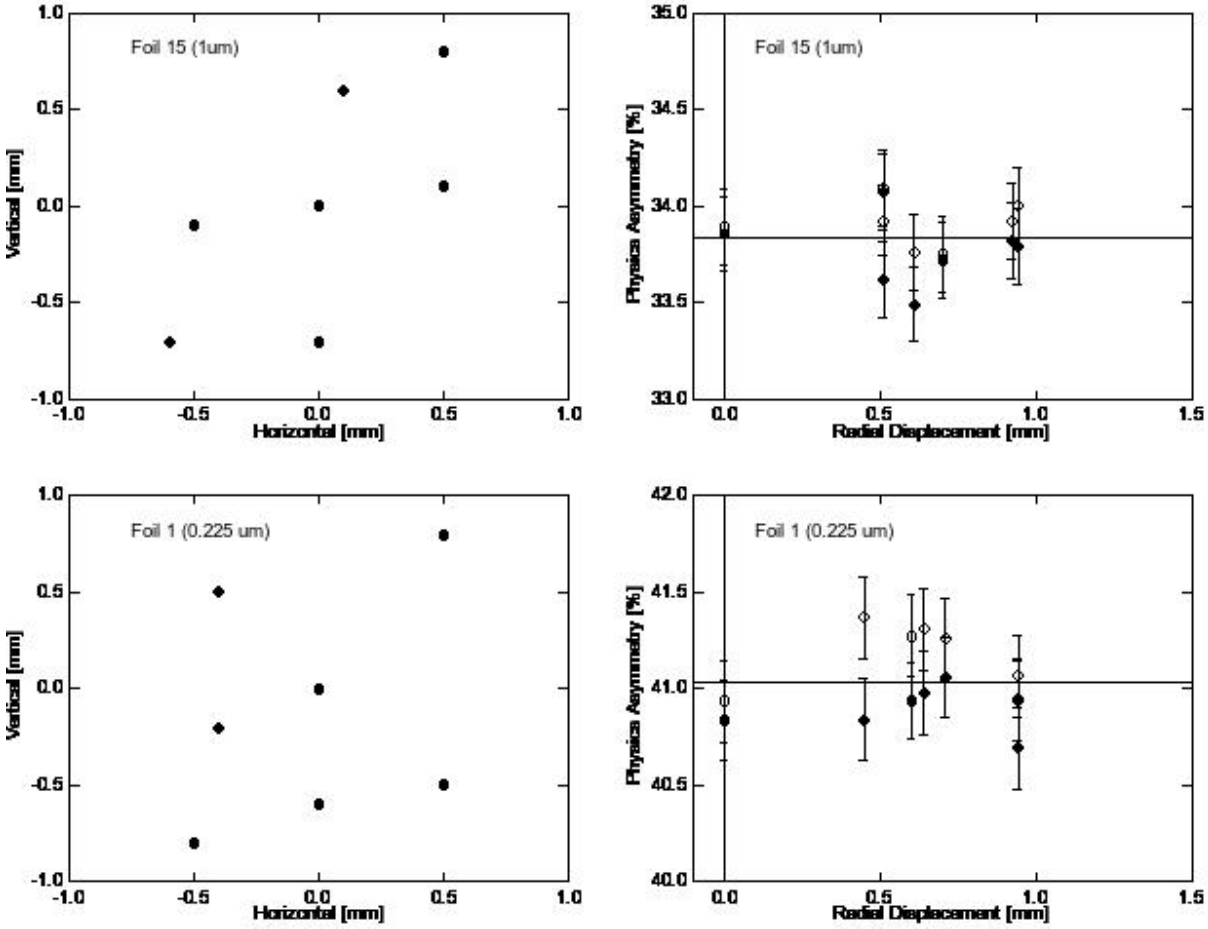

Fig. 7. Physics asymmetry vs. radial position foil #15 (Au: 1.0 μm) and foil #1 (Au: 0.225 μm). The left plots show the position relative to nominal operating point (0,0) and the right plots show a scatter of asymmetry vs. radiation displacement from (0,0).

3 Run II Results

Run II : Asymmetry vs. Beam Energy

The Mott asymmetry as a function of beam energy was studied by varying the gradient R028GSET and minimizing the energy spread with R028PSET of the final SRF cavity. The beam energy was set for four values about the nominal energy. For each energy the Mott physics asymmetry was measured using both foil #15 (Au:1μm) and foil #14 (Au:0.35 μm). The electron beam kinetic energies were carefully measured [1] and are summarized in Table 5 and plotted in Fig. 8.

Table 5. Run II Beam Momentum and Kinetic Energy

R028	Momentum		Kinetic Energy		Mott Runs		Mott Runs	
GSET	P	δP	T	ΔT	Foil #15 (1 μm)		Foil #14 (0.35 μm)	
MV/m	MeV/c	MeV/c	MeV	MeV	In	Out	In	Out
3.350	5.025	0.012	4.540	0.012	8457 8459	8458 8460	8462 8464	8461 8463
3.740	5.219	0.013	4.733	0.012	8445 8447	8446 8448	8450 8452	8449 8451
4.120	5.404	0.013	4.917	0.013	8433 8435	8434 8436	8438 8440	8437 8439
4.500	5.603	0.013	5.115	0.013	8466 8469	8467 8470	8473 8475	8471 8474
4.890	5.785	0.014	5.297	0.014	8477 8479	8478 8480	8482 8484	8481 8483

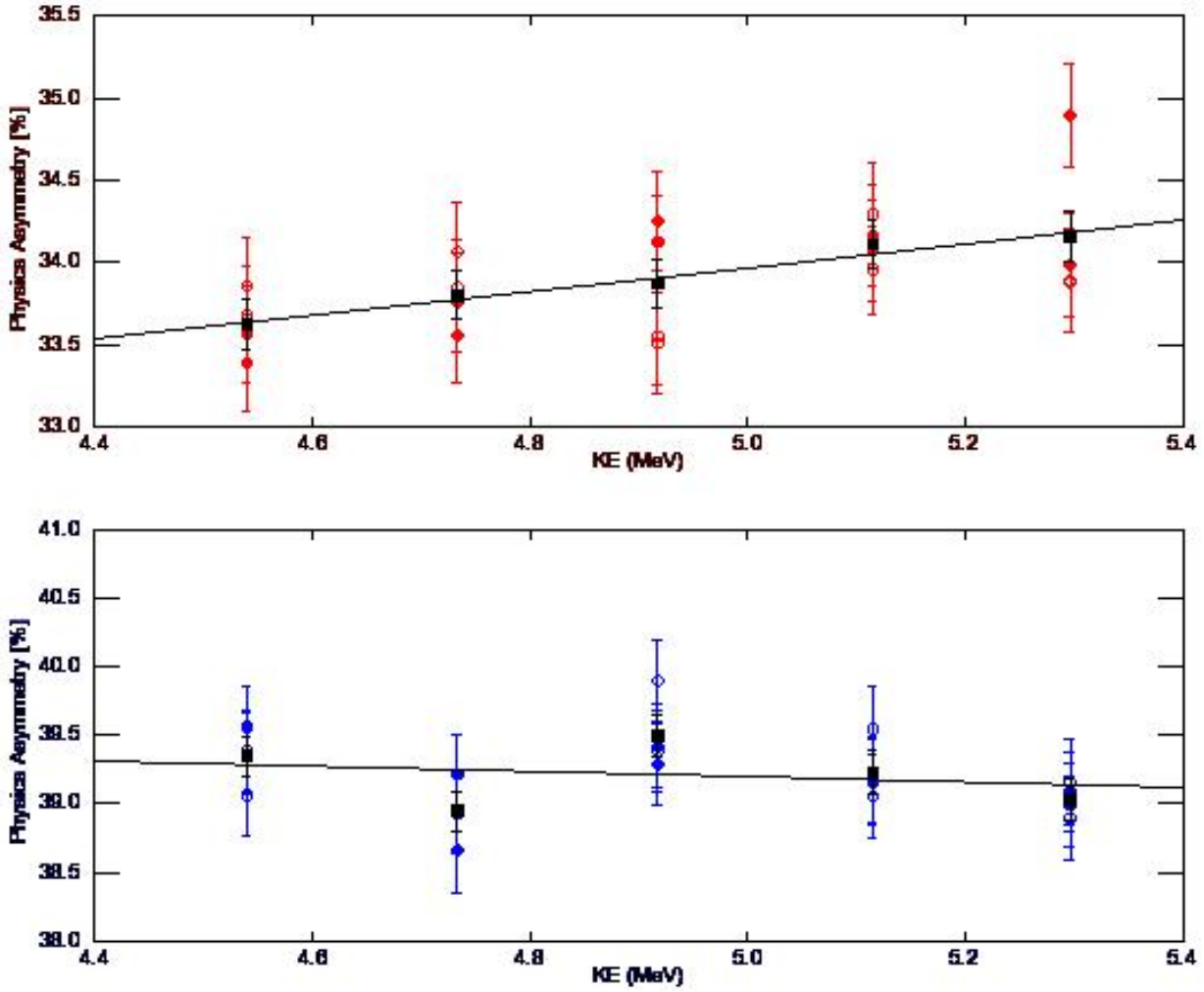

Fig. 7. Physics asymmetry vs. kinetic energy for foil #15 (Au: 1.0 μm) and foil #14 (Au: 0.35 μm). The variation with energy is 0.022/MeV for foil #15 and -0.0046/MeV for foil #14. The variation with asymmetry is consistent with the Sherman function variation with energy in the region of 172.5-173.5 degrees.

4 Reference

1. J. Grames, "*Mott Experiment Run I/II Beam Energies*", JLAB-TN-17-001 (2017).

5 Appendix A

Step 1. The ELOG entry images were saved as PNG files and cropped to 165 x 165 pixels. An example is shown here and summarized for all images below.

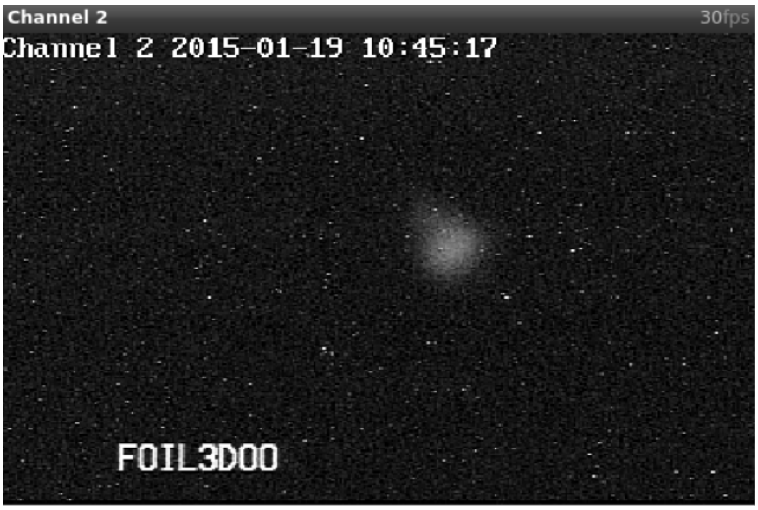

FILENAME	WIDTH	HEIGHT	CEN_X	SIG_X	FWHM_X	CEN_Y	SIG_Y	FWHM_Y
run1-foil15-fig10.png	165	165	114.5	12.9	30.5	95.2	18.6	43.9
run1-foil15-fig11.png	165	165	46.4	13.2	31.0	97.0	12.0	28.2
run1-foil15-fig1.png	165	165	47.2	13.8	32.6	117.7	14.5	34.2
run1-foil15-fig5.png	165	165	61.9	12.5	29.5	107.5	19.0	44.7
run1-foil15-fig6.png	165	165	99.4	13.2	31.0	75.8	14.1	33.3
run1-foil15-fig7.png	165	165	80.2	13.8	32.4	93.2	13.8	32.6
run1-foil15-fig8.png	165	165	65.2	13.9	32.6	78.6	16.4	38.6
run1-foil15-fig9.png	165	165	97.4	12.9	30.4	109.8	16.4	38.7
run1-foil1-fig10.png	165	165	101.7	15.3	36.0	106.8	17.4	40.9
run1-foil1-fig3.png	165	165	86.0	14.7	34.6	95.4	15.4	36.4
run1-foil1-fig4.png	165	165	121.2	15.3	35.9	92.8	16.5	38.9
run1-foil1-fig5.png	165	165	83.7	15.4	36.4	125.2	18.9	44.4
run1-foil1-fig6.png	165	165	52.1	15.6	36.7	99.4	14.5	34.2
run1-foil1-fig8.png	165	165	86.2	14.2	33.5	62.6	14.7	34.6
run1-foil1-fig9.png	165	165	102.4	14.4	34.0	78.8	17.6	41.6

Step 2. The true beam position at the target is reduced in the plane of the target-mirror-camera by the projected distance of the mirror-foil vector relative to the beam axis. This value is estimated from drawings to be 13° from drawings however actual alignment of the mirror and its support fixture may result in a variation by as much as ±6°. This sub-tended image is collected along a target-mirror-camera plane of about 45° cw with respect the horizontal beam plane and is thus

coupled. The image is also inverted by the mirror. Finally, the true beam position (x_b,y_b) is related to the camera pixel position (x_p,y_p) by the following transformation:

$$\begin{pmatrix} x_c \\ y_c \end{pmatrix} = \begin{pmatrix} -1 & 0 \\ 0 & 1 \end{pmatrix}_{Inv} \begin{pmatrix} \cos\phi & -\sin\phi \\ \sin\phi & \cos\phi \end{pmatrix}_{\phi=-45°} \begin{pmatrix} \frac{1}{\cos\theta} & 0 \\ 0 & 1 \end{pmatrix}_{\theta=13°} \begin{pmatrix} x_b \\ y_b \end{pmatrix}$$

$$\begin{pmatrix} x_c \\ y_c \end{pmatrix} = \begin{pmatrix} -0.726 & -0.707 \\ -1.000 & 0.707 \end{pmatrix} \begin{pmatrix} x_b \\ y_b \end{pmatrix}$$

This 2 x 2 matrix is inverted to finally yield true beam position as a function of camera pixels.

$$\begin{pmatrix} x_b \\ y_b \end{pmatrix} = \begin{pmatrix} -0.579 & -0.579 \\ -0.819 & 0.595 \end{pmatrix} \begin{pmatrix} x_c \\ y_c \end{pmatrix}$$

Step 3. On a separate occasion images of the target ladder were saved for small 200 step increments of the target ladder. The transformed position of a specific item may then be calibrated to the known physical motion of 4464 ladder steps = 25.4 mm of linear vertical travel. The table below shows the transformed images indicate purely vertical motion of the target ladder and indicate a calibration of 37.9 +/- 1.1 pixels/mm.

Image ABS Pixels		Image REL Pixels		Foil REL Pixels		Ladder ABS Steps	Ladder REL Steps	Ladder (mm)	pixels/mm
-421	476	0	0	0.0	0.0	-73800	0	0	
-392	447	29	-29	0.0	-41.0	-73600	200	1.14	-36.03
-362	419	59	-57	-1.2	-82.2	-73400	400	2.28	-36.13
-329	385	92	-91	-0.6	-129.5	-73200	600	3.41	-37.93
-299	355	122	-121	-0.6	-171.9	-73000	800	4.55	-37.77
-267	322	154	-154	0.0	-217.8	-72800	1000	5.69	-38.27
-235	290	186	-186	0.0	-263.0	-72600	1200	6.83	-38.52
-204	259	217	-217	0.0	-306.8	-72400	1400	7.97	-38.52
-171	226	250	-250	0.0	-353.5	-72200	1600	9.10	-38.83
-140	194	281	-282	0.6	-397.9	-72000	1800	10.24	-38.85

6 Appendix B

An approximation for the average/mean radius of an ellipse's circumference, Er, is the elliptical quadratic mean:

$$Er \approx Er_q = \sqrt{\frac{a^2 + b^2}{2}}.$$

(where a is the central, horizontal, transverse radius/semi-major axis and b is the central, vertical, conjugate radius/semi-minor axis)